

2008

Classification of Cylindrical Targets Buried in Seafloor Sediments

Edit J. Kaminsky

University of New Orleans, ejbourge@uno.edu

Madalina Barbu

University of New Orleans

Follow this and additional works at: https://scholarworks.uno.edu/ee_facpubs



Part of the [Electrical and Electronics Commons](#)

Recommended Citation

Kaminsky, E. and M. Barbu, "Classification of cylindrical targets buried in seafloor sediments," in IEEE Region 5 Tech. Conf., Lafayette, AR, April 20-22, 2007, pp. 117–123.

This Conference Proceeding is brought to you for free and open access by the Department of Electrical Engineering at ScholarWorks@UNO. It has been accepted for inclusion in Electrical Engineering Faculty Publications by an authorized administrator of ScholarWorks@UNO. For more information, please contact scholarworks@uno.edu.

Classification of Cylindrical Targets Buried in Seafloor Sediments

Edit J. Kaminsky and Madalina Barbu
 Department of Electrical Engineering
 University of New Orleans
 New Orleans, LA 70148
 ejbourge@uno.edu
 mbarbu@uno.edu

Abstract—This paper presents the development and evaluation of a time-frequency processing technique for detection and classification of buried cylindrical targets from chirp-based parametric sonar data. The software is designed to discriminate between cylindrical targets—such as cables—of different diameters, which need to be identified as different from other strong reflectors or point targets. The method is evaluated on synthetic data generated with an acoustic scattering model for elastic cylinders for seven different diameters. The model generates characteristic responses of targets acquired by a parametric sonar system. The signal at the sonar receiver hydrophones is first windowed to reduce the data to the region of interest (buried target return). This return is then transformed using joint time-frequency transforms (we use the Wigner and Choi-Williams distributions) to produce a 2D image of the return. Dimensionality reduction and feature extraction are performed by singular value decomposition of this time-frequency image. Linear, quadratic, and Mahalanobis discriminant functions are then applied to the most significant singular values to produce the final classification. The study is carried out for various scenarios of free field response of targets as well as for responses from targets buried in sediment.

I. INTRODUCTION

We address in this paper a challenging classification problem: that of classifying objects buried under sediment in the seafloor. The complexity of the problem arises from factors such as the propagating media, clutter caused by biological sources in the water column, and the fact that acoustic noise in normal incidence-reflection generated by the volume scattering (from inhomogeneities within the sediments) and surface scattering (from roughness of the sediment) is frequently higher than the amplitude of echoes reflected from the buried target of interest.

There are many techniques, particularly pattern recognition methods, employed to solve this type of problems. The signals to be classified should first be transformed into a favorable space by one or more projection methods from which we obtain feature vectors. Among the most frequently used projection techniques are the short time

Fourier transform, principal component analysis (PCA), fractal analysis, and spectra. For the final classification step, some of the frequently encountered techniques are Bayesian classifiers, nonparametric techniques (such as nearest neighbor), hidden Markov models, and neural networks [1].

A pattern recognition approach for classification of buried targets (such as cables) from parametric sonar data is reported in this work. Parametric sonars transmit acoustic signals in the water with a very narrow beam and almost no sidelobes. Parametric sonars have been used in an increasing number of applications in the past years, ranging from traditional seismic processing to more complex systems for object detection and classification [2], [3]. Woodward and Lepper [4] report a study based on an open-water trial using a parametric sonar system with the aim of detecting and classifying embedded or partially embedded objects such as pipelines, lost cargo, and mines. The main finding was that both specular reflections and resonance effects could be observed and they proposed that these could contribute to the classification of targets.

Boulinguez [5] proposed a technique for obtaining a complete identification and localization of objects embedded in sediment. The parametric sonar was used to acquire 3D data on the subbottom area and wavelets were employed for eliminating the noise; high order spectra were used both to improve the range resolution and for classification. Boulinguez also studied object classification using features extracted from the entropy of the Wavelet packet coefficients and from fractal analysis in [6].

Miao introduced in [7] a system which uses principal component analysis for feature extraction and then neural networks for detection and classification of targets in six different optical bands ranging from near UV to near IR. The outputs of the detector/classifier networks in all the channels were fused together in the final decision making system.

Azimi [8],[9] proposed a classification system that consists of a feature extractor using wavelet packets in conjunction with linear predictive coding, a feature selection scheme, and a backpropagation neural network classifier. A multiaspect fusion scheme was also employed for improving the classification performance. Trucco et al. [10], [11] presented a pattern recognition method for the detection of buried objects. The beamformed signals were divided into partially overlapping frames and then projected in the time-frequency space. Features were then extracted and fed into a multivariate Gaussian classifier.

The aim of our current paper is to present a method for buried target classification based on joint time-frequency techniques and singular value decomposition of the transformed image. Of particular interest are long targets such as cables of various diameters, which need to be identified as different from each other and from other strong reflectors or point targets. Synthetic test data are used to exemplify and evaluate our technique. Results illustrate that the proposed algorithm provides accurate ways to classify cylinders of slightly different diameters in various conditions.

We begin by presenting the acoustical model in Section II. The classification algorithm employs a representation of the signal in the joint time-frequency domain, discussed in Section III. The singular value decomposition of the Wigner or Choi-Williams distributions applied to the impulse response is performed next, and summarized in Section IV. The singular value spectrum encodes the time-frequency features of the signal. The first few singular values are the inputs to the classifier. In Section VI, the classification results are shown for the three types of discriminant functions (linear, quadratic, and Mahalanobis) presented in Section V. Conclusions and references follow at the end.

II. ACOUSTIC SCATTERING MODEL

The analysis and results presented in this paper are based on the acoustic scattering model for elastic cylinders presented in [12]. In order to estimate the scattered field due to a cylinder of finite length, the volume flow per unit length of the scattered field of an infinitely long cylinder is integrated over a finite distance. The model was initially proposed to describe scattering of sound by fluid-saturated objects. Many scatters possess elastic properties and conversion of the compressional waves into shear waves is taken into account.

The assumption made for the infinite cylinder is that there is no absorption, dispersion, or nonlinearity in the cylinder or the surrounding medium [12]. The scattering from ends of the cylinder are ignored, and the receiver-

target separation must be great enough to be in the first Fresnel zone (i.e., $L \ll 2\sqrt{r\lambda}$, where L is the length of the cylinder or of the insonified "spot" of a longer cylinder, λ is the acoustic wavelength, and r is the range from the axis of the cylinder to the receiver or field point). Stanton [12] shows that taking into account arbitrary transmitter direction, receiver position and cylinder orientation, and assuming that $r \gg L$, the expression of the scattered pressure at acoustic wavenumber k is given by (1):

$$P_{scatter}(k) = -P_0 \frac{e^{ikr}}{r} \left(\frac{L}{\pi} \right) \frac{\sin(\Delta)}{\Delta} \times \sum_{m=0}^{\infty} \varepsilon_m \sin(\eta_m) e^{-i\eta_m} \cos(m\phi) \quad (1)$$

where P_0 is the amplitude of the incident plane wave, r is the source-target separation, $\Delta = \frac{1}{2}kL(\vec{r}_i - \vec{r}_r) \cdot \vec{r}_c$ (with \vec{r}_r the unit direction of the receiver, \vec{r}_i the unit direction of the incident plane wave, and \vec{r}_c the unit direction of the cylinder axis), ε_m is Neumann's number ($\varepsilon_0 = 1$, $\varepsilon_{m>0} = 2$), η_m is the scattering phase angle, and ϕ is the azimuth angle of the arbitrarily oriented cylinder.

In equation (1), $\frac{\sin(\Delta)}{\Delta}$ represents the beam pattern. We assume a Gaussian beam pattern and an effective length insonified given by $\hat{L} = \sqrt{2\pi}\sigma e^{-s_0/2\sigma^2}$ where s_0 is the distance from the maximum response on the bottom to the closest point of approach of the cylinder. The scattered pressure using a Gaussian beam becomes:

$$P_{scatter}(k) = -P_0 \frac{e^{ikr}}{r} \left(\frac{\hat{L}}{\pi} \right) \frac{1}{\sqrt{2\pi}\Sigma} e^{-s_0/2\Sigma^2} \times \sum_{m=0}^{\infty} \varepsilon_m \sin(\eta_m) e^{-i\eta_m} \cos(m\phi), \quad (2)$$

where $\Sigma = 1/(2\pi\sigma)$.

The following considerations are then incorporated in the model: spherical spreading by replacing P_0 by P_1/r , and the bottom effects. Assuming a flat bottom comprising a homogeneous lossy half-space with sound speed c_s and density ρ_s , the pressure is reduced by $T_{ws}T_{sw}e^{-2\alpha_s z_s}$.

Here, $T_{ws} = 2\rho_s c_s / (\rho_w c_w + \rho_s c_s)$ is the normal incidence plane wave transmission coefficient from water to sediment and $T_{sw} = 2\rho_w c_w / (\rho_w c_w + \rho_s c_s)$ is the normal incidence plane wave transmission coefficient from sediment to water, α_s is the attenuation coefficient in the sediment, z_s is depth of the cylinder below the surface, c_w is the sound speed in water and ρ_w is the density of water. The phase factor is altered by e^{ikr} to account for transmission through the bottom. Hence,

$$P_{scatter}(k) = -P_1 T_{ws} T_{sw} \frac{e^{i(k_w r_w + k_s r_s (1 + i\alpha_s/k_s))}}{(r_w + r_s)^2} \left(\frac{\hat{L}}{\pi} \right) \\ \times \frac{1}{\sqrt{2\pi}} e^{-s_0/2} \sum^2 \sum_{m=0}^{\infty} \varepsilon_m \sin(\eta_m) e^{-i\eta_m} \cos(m\phi), \quad (3)$$

where k_w and k_s are the wavenumbers in the water and sediment, respectively, and r_w and r_s define the path lengths in water and in the sediment.

The solution is for a continuous wave signal of infinite duration. For a band-limited, finite duration pulse, a time series can be created from Fourier synthesis of solutions over a discrete range of wavenumbers k_n , $n = 0, 1, \dots, N$. The impulse response for the j^{th} sample of the time series is given by:

$$h_{scatter}(t_j) = \frac{\Delta k}{N} \sum_{n=n_{min}}^{n=n_{max}} P_{scatter}(k_n) e^{2\pi i(j-1)(n-1)}, \quad (4)$$

where $\Delta k = 2\pi f_s / N c_s$ is the resolution of the wavenumber in the inverse Fourier transform and n_{min} and n_{max} are determined from the upper and lower frequencies in the band.

III. TIME-FREQUENCY ANALYSIS

Time-frequency methods are powerful tools for studying temporal variations in spectral components. The spectrum's time dependency of the return signal could be a strong indicator of the target's acoustic signature.

The generalized time-frequency representation can be expressed in term of the kernel $\varphi(\theta, \tau)$, which determines the properties of the distribution [13]:

$$C(t, \varpi) = \frac{1}{4\pi^2} \int \int \int f^*(u - \tau/2) f(u + \tau/2) \\ \times \varphi(\theta, \tau) e^{-j\theta t - j\tau\varpi + ju\theta} du d\tau d\theta \quad (5)$$

The Wigner distribution can be derived from the generalized time-frequency representation using the kernel $\varphi(\theta, \tau) = 1$:

$$W(t, \varpi) = \frac{1}{2\pi} \int f^*(u - \tau/2) f(u + \tau/2) e^{-j\tau\varpi} d\tau \quad (6)$$

The Wigner distribution function is a time-frequency analysis tool that can be used to illustrate the time-frequency properties of a signal, and it can be interpreted as a function that indicates the distribution of the signal energy in the time-frequency space. The Wigner distribution

is symmetric with respect to the time-frequency domains, it is always real but not always positive. The Wigner distribution exhibits advantages over the spectrogram (short-time Fourier transform): the conditional averages are exactly the instantaneous frequency and the group delay.

One disadvantage of the Wigner distribution is that it sometimes indicates intensity in regions where one would expect zero values. These effects are due to cross terms and can be minimized by choosing a kernel that has the form $\varphi(\theta, \tau) = e^{-\theta^2 \tau^2 / \sigma}$, which yields the Choi-Williams distribution:

$$C(t, \varpi) = \frac{1}{4\pi^{3/2}} \int \int \frac{1}{\sqrt{\tau^2 / \sigma}} f^*(u - \tau/2) f(u + \tau/2) \\ \times e^{-\sigma(u-t)^2 / \tau^2 - j\tau\varpi} du d\tau \quad (7)$$

With this kernel, the marginals are satisfied and the distribution is real. If the parameter σ has a large value, the Choi-Williams distribution approaches the Wigner distribution, as the kernel approaches one. For small values of σ , it satisfies the reduced interference criterion.

IV. SINGULAR VALUE DECOMPOSITION

The Singular Value Decomposition (SVD) of the discrete Wigner distribution W is given by

$$W = U D V^T = \sum_i \sigma_i u_i v_i^T \quad (8)$$

$$\|W\|_F^2 = \sum_i \sigma_i^2, \quad (9)$$

where $D = \text{diag}(\sigma_1, \sigma_2, \dots, \sigma_N)$, with $\sigma_1 \geq \sigma_2 \geq \dots \geq \sigma_N$, is the matrix of singular values, U is a unitary matrix that contains a set of orthonormal output vector directions for W , V^T is a unitary matrix containing the set of orthonormal analyzing basis vectors for W (so that the columns of V are the left singular vectors), and $\|W\|_F$ is the Frobenius matrix norm.

V. DISCRIMINANT FUNCTIONS

Classifiers for which the discriminant functions have well predefined mathematical functional forms are parametric classifiers. A linear classifier uses a linear function of its input to base the decision upon. For a two-class classification problem, one can visualize the operation of a linear classifier as splitting a high-dimensional input space with a hyperplane: all points on one side of the hyperplane belong to one class, while those on the other side belong to the second class. A linear classifier is often used in situations where the speed of classification is an issue. A quadratic classifier separates classes by quadratic surfaces.

The assignment of x is to class ω_i if the discriminant for i is larger than for j :

$$g_i(x) > g_j(x), \quad j \neq i \quad (10)$$

It is more common to define a single discriminant function [1] by

$$g(x) \equiv g_i(x) - g_j(x). \quad (11)$$

In this case the vector x is assigned to class ω_i if $g(x) > 0$. The decision boundary between the classes ω_i and ω_j is obtained when $g(x) = 0$.

For minimum-error-rate classifiers, where the maximum discriminant function corresponds to the maximum *a posteriori* probability, the discriminant function g_i is given by:

$$g_i(x) = \ln p(x|\omega_i) + \ln P(\omega_i) \quad (12)$$

where $p(x|\omega_i)$ represent the conditional densities and $P(\omega_i)$ are the *a priori* probabilities for each class. Assuming the conditional densities are normal, the discriminant function becomes [1]:

$$g_i(x) = -\frac{1}{2}(x - \mu_i)^T \Sigma_i^{-1} (x - \mu_i) - \frac{d}{2} \ln(2\pi) - \frac{1}{2} \log(\Sigma_i) + \log(P(\omega_i)). \quad (13)$$

where μ_i is the d -dimensional mean vector for class i , and Σ_i is the covariance matrix for class i .

The distance

$$D_i = \sqrt{\frac{1}{2}(x - \mu_i)^T \Sigma_i^{-1} (x - \mu_i)}, \quad (14)$$

is the Mahalanobis distance between the vector x and the mean vector for the data in class i .

One of the popular discriminant functions is Fisher's linear discriminant, often used to find the linear combination of features which best separate two or more classes of objects or events. The resulting combinations may be used as a linear classifier.

Assuming we have a set of d -dimensional samples $\{x_1, x_2, \dots, x_N\}$, N_1 of which belong to class ω_1 and N_2 belong to class ω_2 , we seek to obtain the projection y :

$$y = W^T x. \quad (15)$$

The optimum class, w^* , is given by

$$w^* = \arg \max \left\{ \frac{W^T S_B W}{W^T S_w W} \right\} = S_w^{-1} (\mu_1 - \mu_2) \quad (16)$$

where S_w is the within-class scatter matrix and S_B is the between-class scatter:

$$S_w = \sum_{x \in \omega_i} (x - \mu_i)(x - \mu_i)^T \quad (17)$$

$$S_B = \sum_{x \notin \omega_i} (x - \mu_i)(x - \mu_i)^T \quad (18)$$

VI. EXPERIMENTAL SETUP AND RESULTS

The proposed technique is based on a pattern recognition approach and includes a representation of the target impulse response in the time-frequency domain. The technique introduced in this work, and demonstrated through simulation, could employ Fractional Fourier Transform (FrFT) in order to compute the impulse response [14], [15]. FrFT is better suited for chirp sonar applications because it uses linear chirps as basis functions and it has a great potential in sonar signal processing. The singular value decomposition of the Wigner distribution or of the Choi-Williams distribution of the impulse response is applied next. This way, the discriminant features for classification are achieved because the singular value spectrum encodes the relevant features of the signal. These features are mapped into a reduced (3D) dimensional space by keeping only the three most significant singular values. Three types of discriminant functions, namely linear, quadratic, and Mahalanobis are then used for classification.

A block diagram of the process that would be used for field data is shown in Fig. 1, assuming the sonar transmits chirped signals, for which the Fractional Fourier Transform could be employed to approximate the impulse response, as detailed in [14], [16]. For continuous waves signals, the standard Fourier transform—instead of the Fractional Fourier Transform—is used. In the work reported here, the first two blocks are replaced by the generation of the simulated impulse response data from the model discussed in Section II.

Various experiments are simulated for investigating the performance of the proposed target classification method. The shape of the targets is assumed to be cylindrical. In our simulation we used seven target radii: $r_1 = 1.25$ cm, $r_2 = 1.5$ cm, $r_3 = 1.8$ cm, $r_4 = 2$ cm, $r_5 = 2.3$ cm, $r_6 = 2.7$ cm, and $r_7 = 3$ cm which are the seven classes, class 1 through class 7.

The following parameters were initially set: the sound velocity in water, $c_w = 1500$ m/s; the depth of the water is 10 m; the sound velocity in the sediment was first set to 1500 m/s so as to represent free field (i.e., target floating in water), but for testing the velocity in the sediment is $c_s = 1475$ m/s; finally, the burial depth in the sediment (or water) was 25 cm. The generated data consisted of

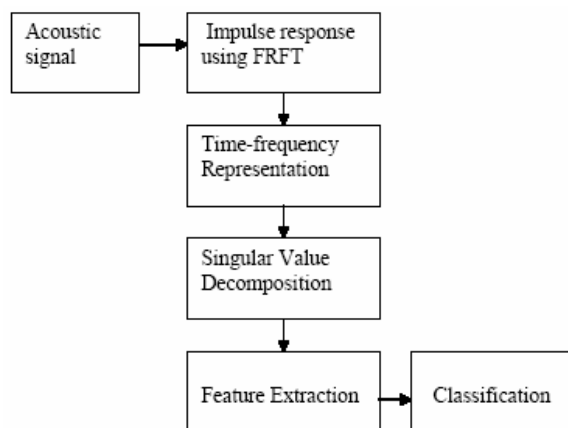


Fig. 1. Processing system for classification of return echoes.

nineteen steps each advancing 0.02 m along track. The first scenario simulated considers the free field (i.e. no sediment) while the next one simulates a muddy bottom.

In the free field case we perform five experiments. In the first experiment we consider a cylinder for which the compressional velocity is $c_c = 3100$ m/s while for the second experiment $c_c = 2800$ m/s. The target is assumed to be at a depth of 25 cm in water. In order to obtain a supervised classification we use a training data set of seventy vectors that correspond to ten odd steps for each of the seven classes. For the testing data set we use sixty-three vectors from the even nine steps. Each 3D feature vector is composed of the 3 largest singular values.

The third experiment (3a through 3c) consisted of training the classifiers with 105 vectors of data from free field (water), but tested with cylinders buried at 15, 35, and 50 cm depth. Experiment 4 (4a through 4c) was used to test the performance when the environmental conditions are changed, by varying the sound velocity in the water from the training value of 1500 m/s to 1520, 1535, and 1550 m/s (caused, for example, by different salinity or temperature); both the training and testing sets contained 105 vectors each.

The sensitivity of the algorithm to the target material was tested in experiment 5. In this experiment, for the free field data the size of the training and testing data was 133 vectors. The target sound velocity for the training data set was $c_c = 2800$ m/s. We use the same depth and three different types of the materials, corresponding to sound velocities $c_c = 2775$ m/s, 2750 m/s, and 2725 m/s.

An evaluation of the proposed classification technique for targets buried in sediment using free field target response data for training and mud target response data

for testing are considered in experiments 6 and 7, where the buried cylinder (corresponding to $c_c = 2800$ m/s) is positioned at two different depths: 15 cm and 25 cm, respectively.

A summary of the parameters for each experiment is given in Table I. Training for all cases is done with free field data with a sound speed in water of 1500 m/s. The burial depth for training was always 25 cm.

The performances of the various classifiers for the free field experiments are presented in Table II.

TABLE I

SUMMARY OF EXPERIMENTAL SETUP FOR ALL SIMULATED EXPERIMENTS. ALL SPEEDS ARE IN M/S AND DEPTH IN M.

Exp No.	Exp Type	Train c_c	Test			
			c_w	c_s	c_c	Depth
1	free	3100	1500	1500	3100	25
2	free	2800	1500	1500	2800	25
3a	free	3100	1500	1500	3100	15
3b	free	3100	1500	1500	3100	35
3c	free	3100	1500	1500	3100	50
4a	free	3100	1520	1500	3100	25
4b	free	3100	1535	1500	3100	25
4c	free	3100	1550	1500	3100	25
5a	free	2800	1500	1500	2775	25
5b	free	2800	1500	1500	2750	25
5c	free	2800	1500	1500	2725	25
6	buried	2800	1500	1475	2800	10
7	buried	2800	1500	1475	2800	25

TABLE II

EXPERIMENTAL RESULTS SHOWING ACCURACY OBTAINED FOR FREE FIELD EXPERIMENTS.

Exp	Linear		Quadratic		Mahalanobis	
	Wigner	C-W	Wigner	C-W	Wigner	C-W
1	71	82	100	100	100	100
2	75	57	100	100	100	100
3a	85	85	100	100	100	100
3b	82	80	100	100	100	100
3c	83	80	100	100	100	100
4a	83	88	100	100	100	100
4b	82	88	100	100	100	100
4c	82	86	97	100	97	100

The quadratic and Mahalanobis based classifiers show similar higher accuracies than the linear classifiers for both Wigner and Choi-Williams distributions. The quadratic and Mahalanobis classifiers tested in free field proved to be robust to the changes in the environmental conditions and burial depth.

The experimental results for the fifth experiment (change in buried target's sound velocity) are presented in Figure 2, where we see that the quadratic based classifier achieved the best accuracy for both Wigner and Choi-Williams distributions. Clearly, as the cylinder's sound velocity departs

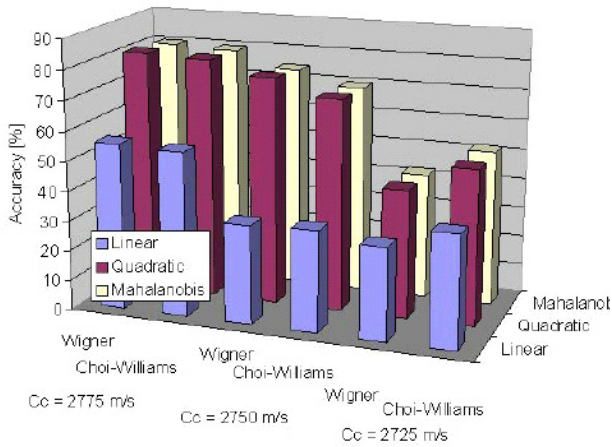


Fig. 2. Classification results showing the sensitivity to the cylinder’s material sound velocity.

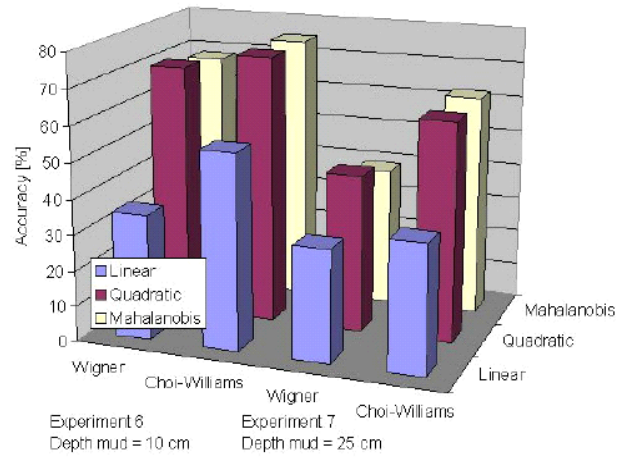


Fig. 3. Classification results showing the sensitivity to burial depth of the cylinder.

from that of the training set, classification performance deteriorates. The Choi-Williams distribution, however, produces better results than the Wiener distribution if the testing velocity is very different from the training velocity.

The cylinders were buried in sediment, with a sound velocity in the sediment of 1475 m/s. The classifiers were designed (i.e., trained) with the target in water (sound velocity of 1500 m/s). 133 signals were used for training, and the same number (but different signals) for testing.

An evaluation of the proposed technique for sediment buried target classification using free field target response data for training and mud target response data for testing are considered in the experiments 6 and 7, where the buried cylinder (corresponding to $c_c = 2800 \text{ m/s}$) is positioned at two different depths : 15 cm and 25 cm, respectively. The classification results for experiments 6 and 7 are illustrated in Figure 3. Both the quadratic and the Mahalanobis based classifiers show considerably higher accuracy than the linear classifier, particularly for the Choi-Williams distribution.

The classification accuracy degrades as the burial depth increases. This is expected because the amplitude and shape of the returned signals get considerably worse as the travel time (or distance) in the sediment gets larger.

An important characteristic of our time-frequency/SVD method is that good classification accuracy of an unknown target (of various materials and buried at various depths) is achieved having only the response of a known target in the free field. A higher classification accuracy is expected for larger differences in target sizes, or smaller differences in the environment. Remember that the accuracies listed

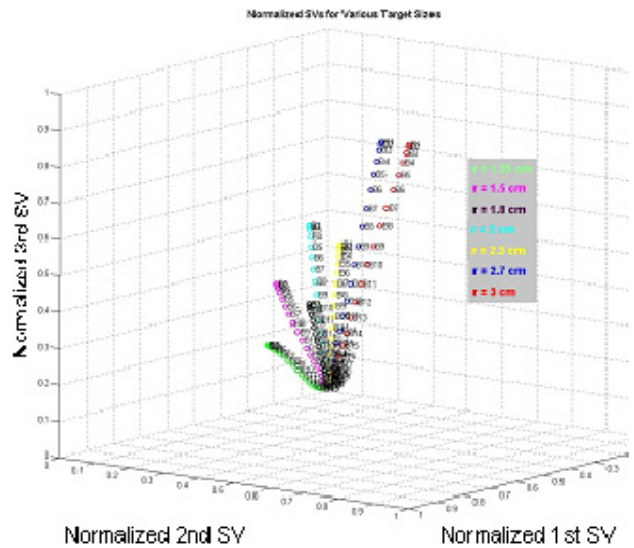


Fig. 4. Singular values of the Wigner distribution of targets of seven different diameters.

and plotted are averages over the 7 classes.

Fig. 4 is used to demonstrate that the singular values of the Wiener distribution of targets of different radii are indeed clearly separable. The numbers on the plots (e.g. B01) indicate the beam number.

VII. CONCLUSIONS

The classification method presented in this paper is based on singular value feature extraction from two time-frequency distributions (Wigner and Choi-Williams) ap-

plied to the target impulse response. Discriminant features for classification are achieved because the singular value spectrum encodes relevant features of the signal. The features obtained were mapped in a reduced (3D) dimensional space, where three classification approaches were employed.

The quadratic and Mahalanobis classifiers show, on average, similar accuracy but superior to the linear classifier under all scenarios. A good accuracy of the proposed method is obtained even when the environmental conditions and the depth of the buried target are varied from the training conditions. Good classification accuracy of an unknown target (of various materials and buried at various depths) is achieved having only the response of a known target in the free field as training data.

The method proved to be effective on synthetic data, simulated for buried targets detected by a parametric sonar. Seven cylindrical targets with various diameters were considered. Tests with actual field data collected with a parametric sonar should be done to verify the results presented here. NRL is planning to collect these data but these were not available at the time of this writing.

VIII. ACKNOWLEDGEMENT

This work was funded by NRL through grant FNRL0005DR00G to the University of New Orleans, Edit Kaminsky Bourgeois, PI. We sincerely thank Drs. D. Bibee and W. Sanders for their contributions to this work.

REFERENCES

- [1] R. O. Duda, P. E. Hart, and D. G. Stork, *Pattern Classification*. China Machine Press, 2004.
- [2] B. Woodward, A. D. Goodson, J. C. Cook, and P. A. Lepper, "Acoustic seabed characteristics using non-linear acoustics," *Proceedings of 2nd European Conference on Underwater Acoustics*, vol. 2, pp. 875–880, Copenhagen, Denmark, 1994.
- [3] —, "A phase steered parametric array for sub bottom profiling," *Proceedings of 6th International Conference on Electronic Engineering in Oceanography*, no. 394, pp. 77–82, Cambridge, MA, 1994.
- [4] B. Woodward and P. A. Lepper, "Acoustic detection and classification on fluid filled cylinders embedded in sediments," *Proceedings of Oceans 2003*, pp. 1912–1916, San Diego, CA, 2003.
- [5] D. Boulinguez, A. Quinquis, and M. Brussieux, "Classification of buried objects using a parametric sonar," *Proceedings of IEEE Oceans 98 Conf.*, vol. 1, pp. 1264–1268, Nice, France, 1998.
- [6] D. Boulinguez and A. Quinquis, "Entropy and fractal analysis for underwater object classification," *Proceedings of 5th European Conference on Underwater Acoustics*, vol. XXIV, pp. 1103–1108, Lyon, France, 2000.
- [7] X. Miao, M. R. Azimi-Sadjadi, B. Tian, A. C. Dubey, and N. H. Witherspoon, "Detection of mine and minelike targets using principal component and neural-network methods," *IEEE Transactions on Neural Networks*, vol. 9, no. 3, pp. 454–463, 1998.
- [8] M. R. Azimi-Sadjadi, Q. Huang, and G. J. Dobeck, "Underwater target classification using multiaspect fusion and neural networks," *Proceedings of SPIE Int. Symp. Aerospace/Defence Sensing Contr.*, pp. 334–341, Orlando, FL, 1998.
- [9] M. R. Azimi-Sadjadi, D. Yao, Q. Huang, and G. J. Dobeck, "Underwater target classification using wavelet packets and neural networks," *IEEE Transactions on Neural Networks*, vol. 11, no. 3, pp. 784–794, 2000.
- [10] A. Trucco and A. Pescetto, "Acoustic detection of objects buried in the seafloor," *Electronics Letters*, vol. 36, no. 18, pp. 1595–1596, 2000.
- [11] A. Trucco, "Detection of objects buried in the seafloor by a pattern recognition approach," *IEEE Journal of Oceanic Engineering*, vol. 26, no. 4, pp. 769–782, 2001.
- [12] T. K. Stanton, "Sound scattering by cylinders of finite length. II. elastic cylinders," *Journal of Acoustic Society of America*, vol. 83, no. 1, pp. 64–67, 1988.
- [13] W. Mecklenbrauker and F. Hlawatsch, *The Wigner Distribution. Theory and Applications in Signal Processing*. Elsevier, 1997.
- [14] M. Barbu, E. Kaminsky, and R. Trahan, "Sonar signal enhancement using fractional fourier transform," *Proceedings of the SPIE Defense and Security Symposium, Automatic Target Recognition XV*, vol. 5807, pp. 170–177, 2005.
- [15] M. Barbu, "Acoustic seabed and target classification using fractional fourier transform and time-frequency transform techniques," Ph.D. Dissertation, University of New Orleans, New Orleans, LA, USA, 2006.
- [16] M. Barbu, E. Kaminsky, and R. Trahan, "Fractional fourier transform for sonar signal processing," *Proceedings MTS/IEEE Oceans 2005 Conf.*, vol. 2, pp. 1630–1635, 2005.